RSC Advances

PAPER

View Article Online
View Journal | View Issue

Cite this: *RSC Adv.*, 2020, **10**, 37982

New cytotoxic natural products from the marine sponge-derived fungus *Pestalotiopsis* sp. by epigenetic modification†

Hui Lei,[a] Dan Zhang,[a] Nan Ding,[c] Siwei Chen,[a] Can Song,[a] Yu Luo,[a] Xiujuan Fu,[a] Xiaoxu Bi*[b] and Hong Niu*[a]

Received 13th August 2020
Accepted 9th September 2020

DOI: 10.1039/d0ra06983c

rsc.li/rsc-advances

Four new polyketide derivatives, pestalotiopols A–D (**1–4**), together with seven known compounds (**5–11**), were isolated from a chemical-epigenetic culture of *Pestalotiopsis* sp. The structures and absolute configurations of the new compounds (**1–4**) were determined by spectroscopic analyses, Mo_2-induced CD, and electronic circular dichroism (ECD) calculations. All the isolated compounds (**1–11**) were tested for their cytotoxic activities. Among these compounds, compounds **1**, **2**, **6** and **7** exhibited cytotoxicity against four human cancer cell lines with IC_{50} values of 16.5–56.5 μM. The structure–activity relationships of compounds (**1–11**) were examined. The results indicated that both the diol system of the side chain and the aldehyde group might contribute to the cytotoxic activity. The possible biosynthetic pathways for compounds (**1–4**) were also postulated.

Introduction

Pestalotiopsis is an asexual genus that is distributed widely in tropical and temperate ecosystems of the earth.[1] *Pestalotiopsis* species had been obtained from diverse environments and were proven to be a rich source of secondary metabolites with unique structural features and diverse pharmacological properties.[2–6] The world's first billion dollar anticancer drug, paclitaxel was isolated from the marine fungus *Pestalotiopsis* sp. reported in 1996.[7] This was followed by the isolation of numerous new compounds with diverse chemical structures from the *Pestalotiopsis* genus.[8–10] Some of these compounds exhibited diverse bioactivities including antitumor, anti-inflammatory, antibacterial, and anti-HCV.[11–14]

Our previous investigation of a *Pestalotiopsis* sp. resulted in the isolation of several new compounds including polyketides,[15] isocoumarins, and sesquiterpenoids.[16] In order to obtain more new bioactive secondary metabolites from species of this genus, a strain of *Pestalotiopsis* sp. was treated with epigenetic modifier including 5-aza-2-deoxycytidine and DNA methyltransferase (RG 108). Application of the epigenetic modifier approach led to the production of four new polyketide derivatives, pestalotiopols A–D (**1–4**), together with seven known compounds, (*S*)-6-(hydroxymethyl)-4-methyl-5,6-dihydro-2*H*-pyran-2-one (**5**),[17] heterocornols A, E, and F (**6**, **7**, and **11**),[15] pestalotiopol B (**8**),[18] dendocarbin B (**9**),[19] 2α-hydroxyisodrimeninol (**10**)[19] (Fig. 1). Herein, details of the isolation, structural elucidation, and bioactivities of these compounds are reported.

Results and discussion

Compound **1** was obtained as white amorphous powder. Its molecular formula was determined to be $C_{12}H_{16}O_4$ based on its HRESIMS spectrum data at *m*/*z* 223.1018 $[M - H]^-$ and ^1H and ^{13}C NMR data. A detailed analysis of its ^1H NMR spectrum (Table 1) data displayed characteristic signals including three aromatic protons of a 1,2,3-trisubstituent benzene [δ_H 6.79 (d, J = 8.0), 7.45 (t, J = 8.0), 6.85 (d, J = 8.0)] and an aldehyde proton at δ_H 10.43 (1H, s). The ^{13}C NMR and HSQC spectra of **1** (Table 1) displayed 12 carbon signals including one methyl, two methylenes, two oxygenated methines, three methines (three olefinic carbons), three nonprotonated carbons, and one aldehyde group at δ_C 197.3. The ^1H and ^{13}C NMR data of **1** were almost identical to those of heterocornol A (**6**) isolated from the same strain,[15] indicating that both compounds had the same planar structures, except for the relative configuration at C-10 and C-11 in **1** and **6**. This result was also confirmed by the chemical shifts of C-8 ($\Delta\delta_C$ −0.2, $\Delta\delta_H$ 0.02/−0.03), C-9 ($\Delta\delta_C$ 0.3, $\Delta\delta_H$ 0.12/−0.07), C-10 ($\Delta\delta_C$ 0.3, $\Delta\delta_H$ −0.02), C-11 ($\Delta\delta_C$ 0.4, $\Delta\delta_H$ −0.09), and C-12 ($\Delta\delta_C$ 0.2, $\Delta\delta_H$ 0.03) compared to the ^1H and ^{13}C NMR data of **6** (Fig. 2) (ESI†). According to the literature, the coupling constant of the same protons are larger than 4 Hz in *erythro* vicinal diols (J > 4.0 Hz) but smaller than 2 Hz in *threo*

[a]*School of Pharmacy, Southwest Medical University, Luzhou, Sichuan 646000, People's Republic of China. E-mail: huilei@swmu.edu.cn*

[b]*College of Agriculture and Life Sciences, Kunming University, Kunming, Yunnan 50241, People's Republic of China*

[c]*Institute of Pathogenic Biology, University of South China, Hengyang 421001, People's Republic of China*

† Electronic supplementary information (ESI) available: 1D and 2D NMR, and HRMS spectra for **1–4**. See DOI: 10.1039/d0ra06983c

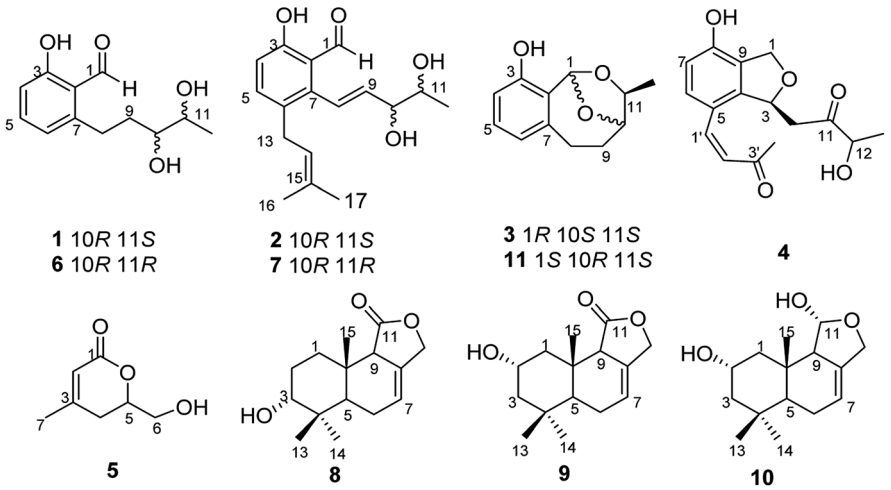

Fig. 1 Structures of compounds **1–11**.

Table 1 ^{1}H (NMR) (600 MHz) and ^{13}C NMR (150 MHz) data for compounds **1–4** in CD_3OD

	1		**2**		**3**		**4**	
No.	δ_C, type	δ_H (J in Hz)	δ_C, type	δ_H (J in Hz)	δ_C, type	δ_H (J in Hz)	δ_C, type	δ_H (J in Hz)
1	197.3, CH	10.43, s	197.7, CH	10.23, s	99.3, CH	6.80, s	70.0, CH_2	4.98, dd (12.3, 2.7), 4.89, d (12.3)
2	119.4, C		118.4, C		126.8, C			
3	164.4, C		161.4, C		154.7, C		80.0, CH	5.91, m
4	116.6, CH	6.79, d (8.0)	115.5, CH	6.79, d (8.6)	113.2, CH	6.62, d (7.2)	143.8, C	
5	138.3, CH	7.45, t (8.0)	137.3, CH	7.35, d (8.6)	128.4, CH	6.96, t (7.2)	119.4, C	
6	122.5, CH	6.85, d (8.0)	131.0, C		121.1, CH	6.60, d (7.2)	128.8, CH	7.44, d (8.4)
7	148.8, C		141.9, C		142.2, C		115.1, CH	6.67, d (8.4)
8	28.9, CH_2	3.25, ddd (14.5, 10.4, 4.6), 3.00, ddd (14.5, 10.1, 6.7)	125.3, CH	6.85, dd (16.1, 1.3)	31.7, CH_2	3.41, td (15.3, 4.2), 1.92, td (15.3, 4.5)	154.5, C	
9	37.2, CH_2	1.94, ddd (13.4, 10.1, 6.6), 1.69, ddd (13.4, 9.8, 4.6)	140.1, CH	5.81, dd (16.1, 6.1)	30.6, CH_2	3.22, ddd (15.9, 12.0, 4.5), 2.64, m	125.6, C	
10	75.9, CH	3.39, ddd (9.0, 5.8, 2.4)	76.2, CH	4.13, ddd (6.4, 5.2, 1.4)	80.8, CH	4.25, dq (6.5, 1.5)	43.8, CH_2	2.87, dd (14.5, 2.9), 2.82, dd (14.5, 3.1)
11	71.7, CH	3.59, dd (6.2, 5.8)	70.2, CH	3.77, qd (6.2, 5.2)	75.9, CH	4.42, qd (6.2, 1.5)	211.2, C	
12	19.1, CH_3	1.19, d (6.2)	17.8, CH_3	1.23, d (6.2)	19.2, CH_3	1.28, d (6.2)	73.1, CH	4.14, m
13							18.2, CH_3	1.24, d (7.0)
1′			30.6, CH_2	3.31, d (7.1)			140.4, CH	7.47, d (6.2)
2′			122.4, CH	5.20, t (7.1)			125.0, CH	6.52, d (6.2)
3′			132.3, C				199.7, C	
4′			16.6, CH_3	1.72, s			26.2, CH_3	2.24, s
5′			24.5, CH_3	1.72, s				

ones (J < 2.0 ppm).[20] Based on the above analysis, the ^{1}H NMR data of **1** revealed that H-10 and H-11 showed the coupling constant of 5.8 Hz, consistent with the known heterocornol A (**6**) (J = 5.1 Hz), indicating that the relative configuration of 10,11-diol corresponded to an *erythro* configuration. The absolute configuration of the *erythro*-10,11-diols in **1** was determined using $Mo_2(AcO)_4$-induced circular dichroism. The circular dichroism (CD) spectrum of **1** showed positive Cotton effect at

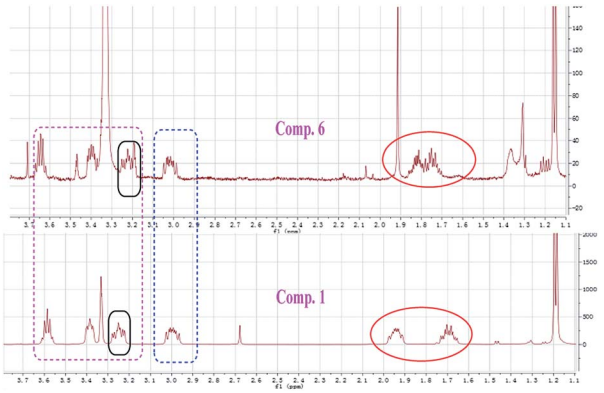

Fig. 2 Comparison of ^{1}H NMR spectra of compounds **1** and **6** from δ_H 1.1 to 3.7 ppm.

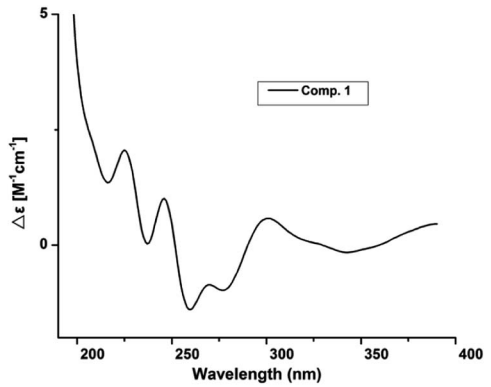

Fig. 3 $Mo_2(AcO)_4$-induced CD spectra of **1**.

305 nm (Fig. 3), while the CD spectrum of **6** gave the negative Cotton effect at 325 nm according to the ref. 15. Additionally, the absolute configuration of the known heterocornol A (**6**) was determined using X-ray and $Mo_2(AcO)_4$-induced circular dichroism method. In order to verify the proposed structure, compound **1** was subjected to electronic circular dichroism (ECD) spectra analysis on the two possible conformers (10*R*,11*S*)-**1** and (10*S*,11*R*)-**1**. The calculated ECD curve of (10*R*,11*S*)-**1** matched well with the experimental curve of **1** (ESI, Fig. S59†). Therefore, the absolute configuration of C-10 and C-11 in **1** could be assigned to be 10*R*,11*S*.

Compound **2** had the molecular formula of $C_{17}H_{22}O_4$, as established by HRESIMS at *m*/*z* 289.1493 $[M - H]^-$ (calcd for $C_{17}H_{21}O_4$, 289.1440). Analysis of the NMR data (Table 1) of **2** revealed that it was very similar to those of vaccinol G (**7**),[21] except some of the chemical shifts changed, C-9 (δ_C 140.1), C-10 (δ_C 76.2), C-11 (δ_C 70.2), and C-12 (δ_C 17.8) in **2**, which was confirmed by the HMBC correlations from H-1′ (δ_H 3.31) to C-5 (δ_C 137.3), C-6 (δ_C 131.0), C-7 (δ_C 141.9), C-2′ (δ_C 122.4) and from H-8 (δ_H 6.85) to C-6 (δ_C 131.0), C-2 (δ_C 118.4), C-7 (δ_C 141.9), and C-10 (δ_C 76.2), together with the COSY correlations H-8/H-9/H-10/H-11/H-12 and H-4/H-5 (Fig. 6). While determining the configurations of C-10 and C-11 during storage for one week. Interestingly, compound **2** could convert to two compounds (**2** and **7**) when kept at room temperature in CD_3OD, while the separation of **2** and **7** by HPLC chromatographic methods was successful (ESI†). This results suggested **2** and **7** differed in the configuration at the vicinal diol side strain, which closely resembled those of **1** and **6**. The analogous chemical shifts and coupling constants of **2** (J = 5.2 Hz) and **1** (J = 5.8 Hz) and indicated that **2** possessed the same relative configuration as **1**. Considering the probable biosynthetic pathway, the absolute configurations of compound **2** was assigned as shown in Fig. 1. The $Mo_2(AcO)_4$-induced circular dichroism spectrum helped reconfirm the absolute configurations of compound **2** (Fig. 4). This assignment was further confirmed by ECD calculations, and the absolute configurations of **2** were determined as 10*R*,11*S* (ESI, Fig. S60†).

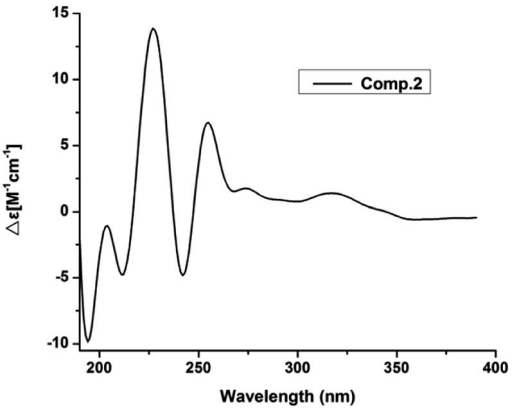

Fig. 4 $Mo_2(AcO)_4$-induced CD spectra of **2**.

Compound **3** was isolated as a white amorphous solid. The molecular formula was established to be $C_{12}H_{14}O_3$ by HRESIMS. Analysis of the NMR data of **3** revealed that it possessed the similar structural characteristics with **11**. The main difference occurred at the configuration of C-1, C-10, and C-11, which were proved by the carbon chemical shifts of C-1 ($\Delta\delta_C$ 0.5 ppm), C-10 ($\Delta\delta_C$ 3.7 ppm), C-11 ($\Delta\delta_C$ 0 ppm), C-12 ($\Delta\delta_C$ 8.1 ppm), and C-9 ($\Delta\delta_C$ 3.2 ppm) in **3** (ESI†). The planar structure of **3** was confirmed by HSQC, COSY, and HMBC experiments (Fig. 6).

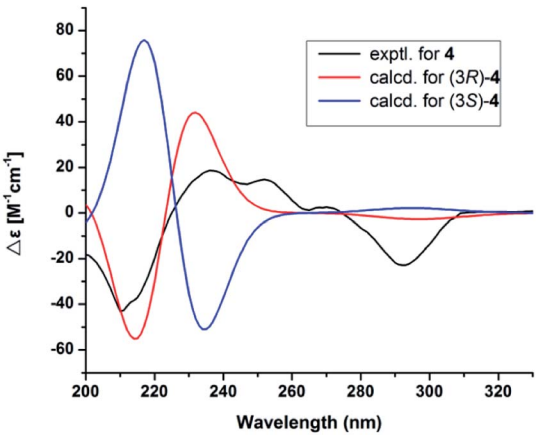

Fig. 5 Electronic circular dichroism (ECD) spectra of **4**.

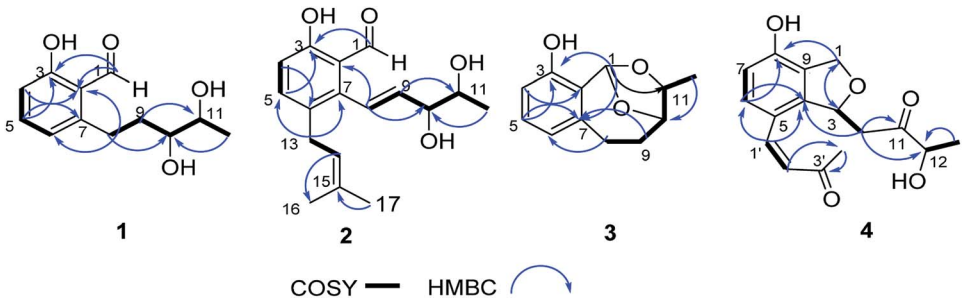

Fig. 6 $^{1}H-^{1}H$ COSY and HMBC correlations of **1–4**.

The relative configuration of **3** was determined by comparing the NMR data and the coupling constant with those of cladoacetals A and B.[22] In addition, considering the possible biosynthesis of compounds **3**, **11** and cladoacetals A and B, it was suggested that **3** had the same configuration as cladoacetal A. Moreover, the absolute configuration of cladoacetal A was determined using X-ray and total syntheses.[23] The absolute configurations of **3** were determined as 1*R*,10*S*,11*S*, by comparing the calculated ECD spectrum with its experimental values. Thus, the structure of **3** was assigned, and named pestalotiopol C.

Compound **4** had the molecular formula $C_{16}H_{18}O_5$ as indicated by the HRESIMS signal at *m*/*z* 313.1061 $[M + Na]^+$ (calcd for $C_{16}H_{18}NaO_5$, 313.1052). The ^{1}H and ^{13}C NMR data of **4** were very similar to those of (*R*)-3-hydroxy-1-[(*R*)-4-hydroxy-1,3-dihydroisobenzofuran-1-yl]butan-2-one,[24] except for the presence of the double bond and carbonyl group of the side chain at C-5, which was confirmed by the HMBC correlations (Fig. 5) of H-1′ (δ_H 7.47) with C-6 (δ_C 128.8), C-4 (δ_C 143.8), C-5 (δ_C 119.4), C-2′ (δ_C 125.0), and C-3′ (δ_C 199.7), together with the $^{1}H-^{1}H$ COSY correlations of H-1′ (δ_H 7.47)/H-2′ (δ_H 6.52). The $^{1}H-^{1}H$ COSY correlations of H-12 (δ_H 4.14) with H-13 (δ_H 1.24) revealed that the hydroxy group was located on C-12 in **4**. In addition, the configuration of the double bond of **4** was confirmed as *Z* geometry based on the coupling constant values between H-1′ and H-2′ ($J_{H1'/2'}$ = 6.2 Hz). The shared biogenesis and similar NMR data (Table 1) suggested that **4** had the same configurations for C-3 as those of (*R*)-3-hydroxy-1-[(*R*)-4-hydroxy-1,3-dihydroisobenzofuran-1-yl]butan-2-one.[24] CD spectra showed a negative Cotton effect at 210 nm of **4** (Fig. 5) suggesting a 3*R* configuration of **4**.[25] Additionally, the absolute configurations of **4** were further determined as 3*R*, by comparing the calculated electronic circular dichroism (ECD) spectrum (Fig. 5). Due to the chiral center C-12 in **4** was far from the chromophore, and only few derivatives were reported.[24] It was difficult to clarify the absolute configurations. We tried to use the modified Mosher's method. Unfortunately, it was unsuccessful because of limited amount available of the compound **4**. Thus, the structure of compound **4** was assigned as shown and named pestalotiopol D.

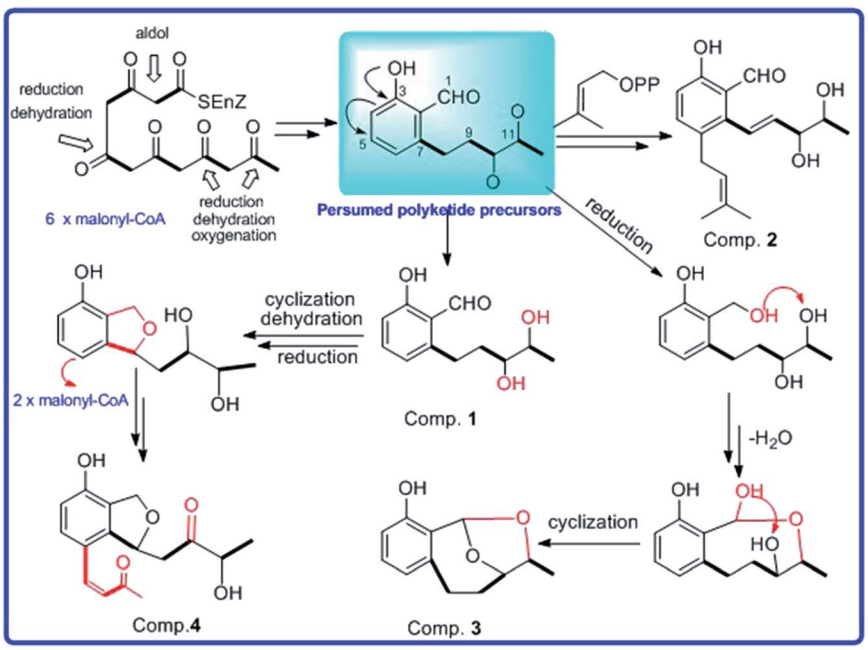

Scheme 1 Possible biosynthetic pathways between compounds **1–4**.

Table 2 Cytotoxic activities of compounds **1–11** (half maximal inhibitory concentration, IC_{50} in μM)

Comp.	BGC-823	SMMC-7721	Ichikawa	7860
1	33.1	25.7	24.8	28.3
2	42.6	52.1	16.5	24.7
3	>100	>100	>100	>100
4	>100	>100	>100	>100
5	>100	>100	>100	>100
6	34.6	26.5	23.6	26.1
7	46.2	56.5	17.8	23.5
8	>100	>100	>100	>100
9	>100	>100	>100	>100
10	>100	>100	>100	>100
11	>100	>100	>100	>100
Adriamycin	1.48	2.24	1.2	2.0

By comparing their NMR data and physicochemical properties with reported ones, the structures of known compounds **5–11** were identified. In addition, the possible biosynthetic pathway for compounds (**1–4**) were also postulated (Scheme 1). Compounds **1–4** were assumed to be biogenetically derived from presumed polyketide precursors through successive reactions such as cyclization, reduction, oxidation, and dehydration. Presumed polyketide precursors was considered to be derived from the malonyl-CoA by cyclization, reduction, oxidation, and dehydration to form an intermediate.

Biological activities

All of the compounds (**1–11**) were evaluated for their cytotoxic activities against four human cancer cell lines (Table 2). Compounds **1**, **2**, **6**, and **7** exhibited cytotoxicity against four human cancer cell lines with IC_{50} values of 16.5–56.5 μM. Unfortunately, the others didn't display cytotoxicities against four human cancer cell lines at 100 μM.

Experimental section

General experimental procedures

Optical rotations were determined using a PerkinElmer 341 automatic polarimeter. Ultraviolet (UV) spectra were measured with a UV-2550 spectrophotometer (Shimadzu Corporation, Tokyo, Japan). IR spectra were measured on a Bruker Tensor 27 FT-IR spectrometer (film). ^{1}H and ^{13}C NMR, DEPT, and 2D NMR spectra were carried out on a Bruker AV-600 spectrometer using TMS as internal standard, δ in ppm rel. HRESIMS (including ESIMS) were recorded on a Bruker maXis TOF-QII mass spectrometer (Bruker Fällanden, Switzerland). Column chromatography (CC) were performed on silica gel (100–200 mesh, 300–400 mesh, Qingdao Marine Chemical Ltd., Qingdao, China), Sephadex LH-20 (GE Healthcare Bio-sciences AB, Sweden), YMC GEL ODS-A (S-50 μm, 12 nm) (YMC Co., Ltd, Kyoto, Japan). Semi-preparative HPLC separations were performed using an ODS column (YMC-ODS-A, 250 × 20 mm, 5 μm). Circular dichroism (CD) spectra were recorded on a Chirascan circular dichroism spectrometer (Applied Photophysics).

Fungal material

The fungal strain *Pestalotiopsis* sp. was isolated from the sponge *Phakellia fusca* that was collected from Xisha Islands of China. The strain was identified according to its DNA amplification and an ITS region sequence analysis (GenBank database). A voucher specimen (no. XWS03F09) was deposited in the School of Pharmacy, Southwest Medical University, Luzhou, Sichuan, China.

Fermentation, extraction, and isolation

The fungal strain *Pestalotiopsis* sp. was grown at 28 °C without shaking for 60 days in one hundred 1000 mL conical flasks containing solid rice medium (each flask contained 200 g of rice, 3 g of artificial sea salt, 10 μM of 5-aza-2-deoxycytidine, 10 μM of RG 108, and 200 mL of distilled water). The whole solid cultures were extracted with EtOAc four times at room temperature. The EtOAc solutions were concentrated under reduced pressure to afford 175 g of crude extract.

The crude extract was subjected to silica gel column chromatography (CC) eluting with a PE and EtOAc mixed solvent system in a step gradient (50 : 1 to 0 : 1, v/v) to yield 9 fractions (Frs 1–9). Fraction 3 was isolated by CC on silica gel eluted with PE-EtOAc (10 : 1 to 0 : 1, v/v) to afford five subfractions (Frs 3.1–3.5). Fr. 3.2 was divided into three subfractions (Frs 3.2.1–3.2.3) by Sephadex LH-20 chromatography (MeOH). Fr. 3.2.3 was further separated by HPLC (75%, MeOH–H_2O) to give **2** (5.0 mg) and **7** (3.0 mg). Fr. 3.3 was subjected to a Sephadex LH-20 column eluting with MeOH, followed by semi-preparative HPLC (75%, MeOH–H_2O) to yield **1** (5.0 mg) and **6** (4.0 mg). Fr. 3.4 was further separated by ODS CC, eluting with MeOH–H_2O (60%) to yield **5** (10.0 mg). Fraction 4 was separated using silica gel column chromatography eluting with PE-acetone (10 : 1) to yield four subfractions (Frs 4.1–4.4). Fr. 4.2 was further purified by HPLC (60%, MeOH–H_2O) to afford **3** and **11** (8.0 mg). Fraction 5 was subjected to Sephadex LH-20 chromatography (MeOH) and further purified by semi-preparative HPLC (60%, MeOH–H_2O) to give **4** (3.0 mg). Fraction 6 was isolated by CC on silica gel eluted with CH_2Cl_2–acetone (15 : 1 to 0 : 1, v/v) to yield six subfractions (Frs 6.1–6.6). Fr. 6.2 was further divided into three subfractions (Frs 6.2.1–6.2.3) by ODS column chromatography eluting with MeOH–H_2O (70 : 30). Fr. 6.2.2 was directly separated by semi-preparative HPLC (60%, MeOH–H_2O) to afford **8** (5.0 mg), **9** (2.0 mg) and **10** (2.0 mg).

Pestalotiopol A (1). White amorphous solid; $[\alpha]_D^{25}$ +16 (*c* 0.30, MeOH); UV (MeOH) λ_{max} (log ε) 258 (3.45), 322 (3.20) nm; IR (film) ν_{max} 3329, 2952, 2926, 1680, 1589, 1439, 1348, 1103, 1024, 943, 849 cm^{-1}; ^{1}H NMR and ^{13}CNMR data, see Table 1; HRESIMS *m*/*z* 223.1018 $[M - H]^-$ (calcd for $C_{12}H_{15}O_4$, 223.0970).

Pestalotiopol B (2). White amorphous powder; $[\alpha]_D^{25}$ +21 (*c* 0.60, MeOH); UV (MeOH) λ_{max} (log ε) 230 (3.61), 345 (3.28) nm; IR (film) ν_{max} 3334, 2948, 2837, 1661, 1539, 1452, 1409, 1350, 1268, 1225, 1110, 1015, 943 cm^{-1}; ^{1}H NMR and ^{13}C NMR data, see Table 1; HRESIMS *m*/*z* 289.1493 $[M - H]^-$ (calcd for $C_{17}H_{21}O_4$, 289.1440).

Pestalotiopol C (3). White amorphous solid; $[\alpha]_D^{25}$ −24 (*c* 0.30, MeOH); UV (MeOH) λ_{max} (log ε) 233 (3.60), 350 (3.58) nm; IR

(film) ν_{max} 3381, 2920, 1628, 1603, 1454, 1251, 1128, 1057, 1013, 987 cm^{-1}; ^1H and ^{13}C NMR data, see Table 1; HRESIMS *m*/*z* 229.0937 $[M + Na]^+$ (calcd for $C_{12}H_{14}NaO_3$, 229.0841).

Pestalotiopol D (4). White amorphous powder; $[\alpha]_D^{25}$ −18 (*c* 0.40, MeOH); UV (MeOH) λ_{max} (log ε) 225 (3.65), 284 (3.96) nm; IR (film) ν_{max} 3240, 2922, 2853, 1705, 1606, 1581, 1381, 1349, 1266, 1162, 1053, 1007, 949, 835 cm^{-1}; ^1H NMR and ^{13}C NMR data, see Table 1; HRESIMS *m*/*z* 313.1061 $[M + Na]^+$ (calcd for $C_{16}H_{18}NaO_5$, 313.1052).

Cytotoxicity assay

The isolated compounds **1–11** were evaluated for their cytotoxic activities against four human carcinoma cell lines, a human gastric carcinoma cell line (BGC-823), a human hepatocellular carcinoma cell line (SMMC-7721), a human carcinoma cell line (Ichikawa), and a human kidney cancer cell line (7860) in an MTT assay as previously reported.[26] IC_{50} value was defined as a 50% reduction of absorbance from the control assay. Adriamycin was assayed as a positive control.

Conclusions

In summary, four new polyketide derivatives, pestalotiopols A–D (**1–4**), together with seven known compounds (**5–11**), were isolated from a chemical-epigenetic culture of *Pestalotiopsis* sp. Structures of the compounds (**1–4**), including their absolute configurations, were determined by spectroscopic analyses, especially the 2D NMR, Mo_2-induced CD analyses. All the isolated compounds (**1–11**) were evaluated for their cytotoxic activities. Compounds **1**, **2**, **6**, and **7** exhibited cytotoxicity against four human cancer cell lines with IC_{50} values of 16.5–56.5 μM. However, the others were inactive in the cytotoxic activities test at 100 μM. These results suggested that both the diol system of the side chain and the aldehyde group might promoted the cytotoxic activity. Compared to cultures in the same medium without 5-aza-2-deoxycytidine and RG 108, four new compounds **1–4** were obtained by chemical-epigenetic method. These results suggest that the chemical-epigenetic modification enriched the chemodiversity of the marine fungus.

Calculation details of ECD spectra

The calculations of new compounds **1–3** were performed by using the density functional theory (DFT) as carried out in the Gaussian 09. Conformation search were performed with MMFF94S force fields using Maestro 10.2 software. All these conformers were further optimized by the density functional theory method at the B3LYP/6-31G(d) level. The ECD were calculated using density functional theory (TDDFT) at B3LYP/6-31+G(d) level with IEFPCM model. The calculated ECD curves were all generated using SpecDis v 1.53 software.

$Mo_2(AcO)_4$-induced circular dichroism

The experimental methods were the same as described in previous papers.[15]

Conflicts of interest

The authors declare no conflicts of interest.

Acknowledgements

This work was funded by the Open Project of Guangdong Key Laboratory of Marine Materia Medica (LMM2019-2), Applied Basic Research Fund of Luzhou Municipal Government-Southwest Medical University (2018LZXNYD-ZK13), and Joint Special Fund Project for Basic Research of Local Universities in Yunnan Province (2019FH001(044)), Scientific Research Fund of Yunnan Education Department (2019J0570).

References

1 X. Y. Yang, J. Z. Zhang and D. Q. Luo, *Nat. Prod. Rep.*, 2012, **29**, 622–641.
2 Y. X. Li, F. L. Zhang, S. Banakar and Z. Y. Li, *RSC Adv.*, 2019, **9**, 599–608.
3 H. Lei, H. Niu, C. Song, X. J. Fu, Y. Luo, S. W. Chen and D. Zhang, *Biochem. Syst. Ecol.*, 2020, **91**, 104072.
4 X. Q. Yu, W. E. G. Müller, D. Meier, R. Kalscheuer, Z. Y. Guo, K. Zou, B. O. Umeokoli, Z. Liu and P. Proksch, *Mar. Drugs*, 2020, **18**, 129.
5 G. R. N. Rathnayake, N. S. Kumar, L. Jayasinghe, H. S. Araya and Y. Fujimoto, *Nat. Prod. Bioprospect.*, 2019, **9**, 411–417.
6 R. C. José, Z. A. Jade, M. J. Jesús, M. A. Blanca, H. O. Simón and A. R. Enrique, *Org. Lett.*, 2019, **11**, 3558–3562.
7 G. A. Strobel, W. M. Hess, E. Ford, R. S. Sidhu and X. Yang, *J. Ind. Microbiol. Biotechnol.*, 1996, **17**, 417–423.
8 J. Xu, X. B. Yang and Q. Lin, *Fungal Divers.*, 2014, **66**, 37–68.
9 L. Rao, Y. X. You, Y. Su, Y. Liu, Q. He, Y. Fan, F. Hu, Y. K. Xu and C. R. Zhang, *Fitoterapia*, 2019, **135**, 1–8.
10 W. H. Wang, C. Park, E. Oh, Y. J. Sung, J. Lee, K. H. Park and H. Kang, *J. Nat. Prod.*, 2019, **82**, 3357–3365.
11 B. Y. Yang, Q. Y. Tong, S. Lin, J. R. Guo, J. W. Zhang, J. J. Liu, J. P. Wang, H. C. Zhua, Z. X. Hua and Y. H. Zhang, *Phytochem. Lett.*, 2019, **29**, 186–189.
12 C. S. Li, B. J. Yang, J. Turkson and S. G. Cao, *Phytochemistry*, 2017, **140**, 77–82.
13 R. Y. Song, X. B. Wang, G. P. Yin, R. H. Liu, L. Y. Kong and M. H. Yang, *Fitoterapia*, 2017, **122**, 115–118.
14 Z. H. Gao, R. R. Gao, X. R. Dong, Z. M. Zou, Q. Wang, D. M. Zhou and D. A. Sun, *Phytochem. Lett.*, 2017, **19**, 108–113.
15 H. Lei, X. P. Lin, L. Han, J. Ma, K. L. Dong, X. B. Wang, Y. Mu, Y. H. Liu and X. S. Huang, *Phytochemistry*, 2017, **142**, 51–59.
16 H. Lei, X. P. Lin, L. Han, J. Ma, Q. J. Ma, J. L. Zhong, Y. H. Liu, T. M. Sun, J. H. Wang and X. S. Huang, *Mar. Drugs*, 2017, **15**, 69.
17 J. Liu, X. F. He, G. H. Wang, E. F. Merino, S. P. Yang, R. X. Zhu, L. S. Gan, H. Zhang, M. B. Cassera, H. Y. Wang, D. G. I. Kingston and J. M. Yue, *J. Org. Chem.*, 2014, **79**, 599–607.

18 J. Xiao, L. B. Lin, J. Y. Hu, F. R. Jiao, D. Z. Duan, Q. Zhang, H. Y. Tang, J. M. Gao, L. Wang and X. L. Wang, *RSC Adv.*, 2017, **7**, 29071.
19 Y. Sakio, Y. J. Hirano, M. Hayashi, K. Komiyama and M. Ishibashi, *J. Nat. Prod.*, 2001, **64**, 726–773.
20 X. W. Chen, C. W. Li, C. B. Cui, W. Hua, T. J. Zhu and Q. Q. Gu, *Mar. Drugs*, 2014, **12**, 3116–3137.
21 J. F. Wang, X. Y. Wei, X. Lu, F. Q. Xu, J. T. Wan, X. P. Lin, X. F. Zhou, S. R. Liao, B. Yang, Z. C. Tu and Y. H. Liu, *Tetrahedron*, 2014, **70**, 9695–9701.
22 U. Holler, J. B. Gloer and D. T. Wicklow, *J. Nat. Prod.*, 2002, **65**, 876–882.
23 D. S. Hsu and S. C. Lin, *J. Org. Chem.*, 2012, **77**, 6139–6146.
24 J. R. Kesting, L. Olsen, D. Staerk, M. V. Tejesvi, K. R. Kini, H. S. Prakash and J. W. Jaroszewski, *J. Nat. Prod.*, 2011, **74**, 2206–2215.
25 J. F. Wang, X. Y. Wei, X. C. Qin, H. Chen, X. P. Lin, T. Y. Zhang, X. W. Yang, S. R. Liao, B. Yang, J. Liu, X. F. Zhou, Z. C. Tu and Y. H. Liu, *Phytochem. Lett.*, 2015, **12**, 59–62.
26 D. Zheng, L. Han, Y. Q. Li, J. Li, H. Rong, Q. Leng, Y. Jiang, L. X. Zhao and X. S. Huang, *Molecules*, 2012, **17**, 836–842.

